

# Modulation of Tetrachloroethylene-Associated Kidney Effects by Nonalcoholic Fatty Liver or Steatohepatitis in Male C57BL/6J Mice

Joseph A. Cichocki,<sup>\*,1</sup> Yu-Syuan Luo,<sup>\*,1</sup> Shinji Furuya,<sup>\*</sup> Abhishek Venkatratnam,<sup>\*</sup> Kranti Konganti,<sup>†</sup> Weihsueh A. Chiu,<sup>\*</sup> David W. Threadgill,<sup>†,‡</sup> Igor P. Pogribny,<sup>§</sup> and Ivan Rusyn<sup>\*,2</sup>

<sup>\*</sup>Department of Veterinary Integrative Biosciences; <sup>†</sup>Texas A&M Institute for Genome Sciences and Society;

<sup>‡</sup>Department of Molecular and Cellular Medicine, Texas A&M University, College Station, Texas 77843; and

<sup>§</sup>National Center for Toxicological Research, US FDA, Jefferson, Arkansas 72079

<sup>1</sup>These authors contributed equally to this study.

<sup>2</sup>To whom correspondence should be addressed at Department of Veterinary Integrative Biosciences, College of Veterinary Medicine, 4458 TAMU, Texas A&M University, College Station, TX 77843. Fax: (979) 458-2778. E-mail: irusyn@cvm.tamu.edu.

## ABSTRACT

Accounting for genetic and other (eg, underlying disease states) factors that may lead to inter-individual variability in susceptibility to xenobiotic-induced injury is a challenge in human health assessments. A previous study demonstrated that nonalcoholic fatty liver disease (NAFLD), one of the common underlying disease states, enhances tetrachloroethylene (PERC)-associated hepatotoxicity in mice. Interestingly, NAFLD resulted in a decrease in metabolism of PERC to nephrotoxic glutathione conjugates; we therefore hypothesized that NAFLD would protect against PERC-associated nephrotoxicity. Male C57BL/6J mice were fed a low-fat (LFD), high-fat (31% fat, HFD), or high-fat methionine/choline/folate-deficient (31% fat, MCD) diets. After 8 weeks mice were administered either a single dose of PERC (300 mg/kg i.g.) and euthanized at 1–36 h post dose, or five daily doses of PERC (300 mg/kg/d i.g.) and euthanized 4 h after last dose. Relative to LFD-fed mice, HFD- or MCD-fed mice exhibited decreased PERC concentrations and increased trichloroacetate (TCA) in kidneys. S-(1,2,2-trichlorovinyl)glutathione (TCVG), S-(1,2,2-trichlorovinyl)-L-cysteine (TCVC), and N-acetyl-S-(1,2,2-trichlorovinyl)-L-cysteine (NACTCVC) were also significantly lower in kidney and urine of HFD- or MCD-fed mice compared with LFD-fed mice. Despite differences in levels of nephrotoxic PERC metabolites in kidney, LFD- and MCD-fed mice demonstrated similar degree of nephrotoxicity. However, HFD-fed mice were less sensitive to PERC-induced nephrotoxicity. Thus, whereas both MCD- and HFD-induced fatty liver reduced the delivered dose of nephrotoxic PERC metabolites to the kidney, only HFD was protective against PERC-induced nephrotoxicity, possibly due to greater toxicodynamic sensitivity induced by methyl and choline deficiency. These results therefore demonstrate that pre-existing disease conditions can lead to a complex interplay of toxicokinetic and toxicodynamic changes that modulate susceptibility to the toxicity of xenobiotics.

**Key words:** toxicokinetic; toxicodynamic; xenobiotic; steatosis; steatohepatitis.

Human health risk assessors face a considerable challenge when it comes to addressing inter-individual variability of adverse health effects associated with environmental exposures (Zeise *et al.*, 2013). In addition to genetics, sex, and diet, pre-

existing disease states may also affect inter-individual variability. Nonalcoholic fatty liver disease (NAFLD) is a good example of a prevalent chronic disease in the developed countries such as the United States, Germany, and Israel (Browning *et al.*, 2004;

Kuhn et al., 2017; Zelber-Sagi et al., 2006). The global prevalence of NAFLD is estimated to be ~25% (Younossi et al., 2016b), and associated economic burden on health care is substantial (Younossi et al., 2016a). NAFLD is a spectrum of health conditions that initially presents as nonalcoholic fatty liver (NAFL) and that can progress to nonalcoholic steatohepatitis (NASH), a liver disease state characterized by accumulation of fat, inflammation, and cell injury (ballooning) (Chalasani et al., 2012). Even though NAFL is considered a benign form of the disease, subjects with NAFL may be more susceptible to further liver damage by other exposures. Exacerbated liver injury has been demonstrated in rodents with experimental NAFLD that were exposed to vinyl chloride (Lang et al., 2018), methotrexate (Hardwick et al., 2014), or a ubiquitous environmental contaminant tetrachloroethylene (PERC) (Cichocki et al., 2017b).

PERC is a chemical that was extensively used in metal degreasing, as a feedstock in chemical syntheses, or in dry-cleaning (International Agency for Research on Cancer, 2014; U.S. EPA, 2011). PERC is one of the most commonly found contaminants at hazardous waste sites (National Research Council, 2010). In the United States, 90% of the population had detectable levels of PERC in their blood (Jia et al., 2012). PERC exposure has been associated with cancer and non-cancer toxicity, including nephrotoxicity in humans and rodents (Cichocki et al., 2016; U.S. EPA, 2011). Toxicity of PERC in the kidney has been attributed to its tissue-specific metabolism (Cichocki et al., 2016).

Metabolism of PERC is mediated by both cytochrome P450s (CYPs) and glutathione-S transferases (GSTs) in the liver (Lash and Parker, 2001). The oxidative pathway yields trichloroacetate (TCA), a rodent hepatocarcinogen (Bull et al., 1990; Herren-Freund et al., 1987). The glutathione conjugation pathway in the liver forms 1,2,2-trichlorovinyl-L-glutathione (TCVG) which can be transported via circulation to the kidney where it is further metabolized to 1,2,2-trichlorovinyl-L-cysteine (TCVC) (Lash and Parker, 2001). The fate of TCVC is either metabolic activation to reactive species, including cytotoxic TCVC-sulfoxide (Elfarra and Krause, 2007), or detoxification via N-acetyltransferase-mediated formation of N-acetyl-1,2,2-trichlorovinyl-L-cysteine (NACTCVC), a mercapturate that is excreted in the urine in humans and rodents (Lash and Parker, 2001). NACTCVC can also be converted to NACTCVC-sulfoxide, which is another nephrotoxic metabolite both *in vivo* and *in vitro* (Cristofori et al., 2015).

A previous study characterized the toxicokinetics of PERC, as well as its oxidative (TCA) and glutathione conjugation metabolites (TCVG, TCVC, and NACTCVC) in the liver, serum, and urine of mice with various degrees of NAFLD that were exposed to a single dose of PERC (Cichocki et al., 2017a). Interestingly, mice with NAFLD generated higher levels of liver TCA, which in turn resulted in more pronounced liver injury (Cichocki et al., 2017b). Whereas much is known about the oxidative metabolites of PERC, little information is available on the toxicokinetics of glutathione conjugates of PERC *in vivo*. NAFLD resulted in a significant reduction in levels of TCVG, TCVC, and NACTCVC in liver, serum, and urine (Cichocki et al., 2017a); however, the kinetics of PERC glutathione conjugates has not been explored in kidney, a target organ for PERC toxicity. Therefore, we tested the hypothesis that, compared with healthy mice, mice with diet-induced NAFLD would have lower kidney concentrations of TCVG, TCVC, and NACTCVC following exposure to PERC, and this reduction in metabolite concentration would be associated with decreased sensitivity to PERC-associated nephrotoxicity.

## MATERIALS AND METHODS

**Chemicals.** PERC (CAS 127-18-4) was obtained from Sigma Aldrich (Cat No. 270393, Batch No. SHLFD9374V, purity 99.93%; St. Louis, Missouri). NACTCVC (purity: 99.7%) was obtained from Toronto Research Chemicals (Toronto, Canada). TCVG (purity: 98.9%), TCVC (purity: 98.4%), 22-amino-5-[(1-[(<sup>13</sup>C)carboxy (<sup>13</sup>C)methyl](<sup>15</sup>N)amino)-1-oxo-3-[(trichloroethenyl)sulfanyl] propan-2-yl)amino]-5-oxopentanoic acid (TCVG\*, purity: 90.4%), 2-(<sup>15</sup>N)amino-3-[(trichloroethenyl)sulfanyl](<sup>13</sup>C<sub>3</sub>)propanoic acid (TCVC\*, purity: 97.5%), and 2-[acetyl(<sup>15</sup>N)amino]-3-[(trichloroethenyl)sulfanyl] (<sup>13</sup>C<sub>3</sub>)propanoic acid (NACTCVC\*, purity: 99.0%) were graciously provided by Dr Avram Gold at the University of North Carolina at Chapel Hill. Other chemicals were of the highest purity available and were from Sigma Aldrich.

**Animals.** The in-life portion of this study has been previously described in Cichocki et al. (2017a). Briefly, 5-week-old male C57BL/6J mice (*n* = 150) were obtained from the Jackson Laboratory (Bar Harbor, Maine) and acclimatized for 1 week on a standard rodent chow containing 4% calories from fat (low-fat diet; LFD; Teklad Rodent Diet #8604; Harlan, Madison, Wisconsin). Mice were randomly assigned (five mice per cage) into groups fed a control LFD, a diet containing 31% calories from fat (high-fat diet, HFD; Diet #519567; Dyets, Inc, Bethlehem, Pennsylvania), or a diet depleted in methionine and devoid of choline and folate (methyl and choline-deficient diet based on HFD, MCD; Diet #519541; Dyets). The overall study design is shown in Figure 1 and the study aimed to model conditions of (1) healthy liver and (2) mild, or (3) severe NAFLD phenotypes.

**Toxicokinetic study design.** Following 8 weeks of feeding with the aforementioned diets, mice were exposed to a single dose of PERC (300 mg/kg in 5% Alkamuls-EL620 in saline; 5 ml/kg). All exposures took place between 07:00 and 10:00 h. Mice (*n* = 5/diet/time-point) were euthanized at 1, 2, 4, 12, or 24 h after gavage (total *n* = 75). An additional four mice per diet group were individually housed in stainless steel metabolic cages with wire mesh bottoms (Techniplast, Chester, Pennsylvania) for 36 h for urine collection (total *n* = 12). Five mice per diet were treated with vehicle and euthanized at 24 h post gavage to perform additional biochemical analyses (total *n* = 15). Serum was prepared from blood drawn at exsanguination via centrifugation (Z gel tubes; Sarstedt, Nümbrecht, Germany). Terminal body weight was recorded. Kidneys were excised, rinsed in saline, blotted dry, weighed, snap-frozen in liquid nitrogen, and stored at -80°C until analyzed.

**Toxicodynamic study design.** After 8 weeks of feeding with the diets above, mice were intragastrically administered a single dose of PERC (300 mg/kg/d in 5% Alkamuls-EL620 in saline, 5 ml/kg) or vehicle for 5 consecutive days (*n* = 8/diet/treatment). This dose was selected as the toxicokinetics of PERC and TCA in male mice after exposure to 150–1000 mg/kg PERC has been characterized in liver and blood and was shown to be well-tolerated in acute (Philip et al., 2007) and sub-chronic studies (National Toxicology Program, 1977). All exposures took place between 07:00 and 10:00 h. Three days prior to necropsy, animals were administered 5-bromo-2'-deoxyuridine in drinking water (0.02%, w/v). At 4 h following the last dose of PERC, animals were deeply anesthetized with pentobarbital (50 mg/kg, i.p.) and euthanized via exsanguination through the vena cava. This time point was selected based on our previously published

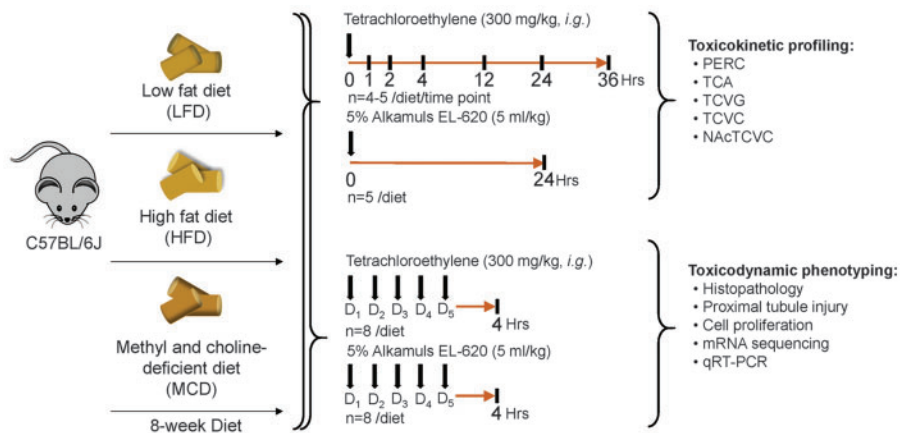


**Figure 1.** Schematic representation of study designs. Adult male C57BL/6J mice were fed with low-fat diet (LFD), high-fat diet (HFD), or methionine and choline-deficient diet (MCD) for 8 weeks, and then intragastrically dosed with tetrachloroethylene (PERC). The first study investigated the toxicokinetics of PERC metabolites up to 36 h after a single dose of PERC (300 mg/kg). The second study examined the toxicodynamic phenotypes of mice administered with repeated doses for 5 consecutive days (300 mg/kg/d); samples were collected 4 h after the last dose. Vertical lines indicate the time points of sample collections. Down arrows represent chemical treatments. Collected endpoints in each study are shown as a bulleted list.

toxicokinetic data showing that PERC and its oxidative and conjugative metabolites were detectable in mouse liver and serum 4 h following a single dose of PERC (Cichocki *et al.*, 2017a). Mice were euthanized, and serum and kidneys were harvested as described above. Terminal body weight and organ weights were recorded. A small section of one kidney was fixed in formalin for histological examination.

**Analysis of PERC and TCA via gas chromatography/mass spectrometry.** PERC and TCA were measured in kidney tissue as previously described in [Cichocki et al. \(2017c\)](#). Briefly, methanolic kidney homogenates were analyzed for PERC via purge-and-trap (dynamic) headspace gas chromatography/mass spectrometry (GC/MS). TCA was analyzed via a modified US EPA Method (EPA 815-B-03-002). Briefly, aqueous kidney homogenates were incubated with 10% (v: v) sulfuric acid in methanol (50°C, 2 h) to generate TCA methyl ester. After liquid-liquid extraction, the derivatives were analyzed via GC/MS.

**Liquid chromatography/mass-spectroscopy (LC/MS) analysis of TCVG, TCVC, and NACTCVC.** Previously detailed method (Luo *et al.*, 2017) was used for detection of TCVG, TCVC, and NACTCVC in kidneys. Briefly, kidney homogenates were subjected to liquid-liquid extraction, and solid-phase extraction prior to chromatographic separation and detection via LC/MS-MS.

**Serum clinical chemistry.** Blood urea nitrogen (BUN) and serum creatinine levels were measured in serum samples using a VetScan 2 (Abaxis, Union City, California) and a Comprehensive Diagnostic Profile rotor according to the manufacturer's instructions.

**Histopathology.** Kidney samples collected from the toxicodynamic study were further examined by histopathology and immunohistochemical staining of kidney injury molecule-1 (KIM-1). Kidney samples were embedded in paraffin, sectioned at 5  $\mu$ m, and stained with hematoxylin and eosin (H&E). A veterinary pathologist who was blinded to the experimental design and sample identification numbers evaluated the slides.

**Immunohistochemical staining of KIM-1.** Tissues were sectioned at 5  $\mu$ m onto poly-L-lysine-coated slides. Deparaffinized and

rehydrated slides were hydrolyzed with warm (37°C) 2N HCl for 20 min in an oven. Slides were rinsed with water (1 min) and then placed in pre-warmed water in a 37°C oven for 20 min. Samples were then incubated in pre-warmed pepsin solution (2g/500 ml of 0.2N HCl; Dako, Santa Clara, California) for 15 min at 37°C. Slides were rinsed with water twice (1 min each), and then with phosphate-buffered saline with 0.1% Tween-20 (PBS-T) twice (3 min each). Endogenous peroxidase activity was blocked using a Peroxidase Blocking Reagent (Dako) for 5 min. After washing with PBS-T, slides were incubated for 10 min at room temperature with a goat anti KIM-1 antibody (1 µg/ml; AF1817, Lot KCA0415031; R&D systems, Minneapolis, Minnesota) prepared in an Antibody Diluent (Dako). After washing with PBS-T, slides were incubated with rabbit anti-goat HRP-conjugated secondary antibody (1:200 dilution; 10 min at room temperature), washed with PBS-T again, and then incubated with 3,3'-diaminobenzidine reagent (Dako) for 8 min at room temperature. After ample washing in deionized water, slides were placed in Mayer's Hematoxylin (1 min), and then thoroughly washed under running tap water. Slides were dehydrated, mounted using Permout (Thermo Fisher Scientific, Waltham, Massachusetts), and examined using light microscopy. Approximately 250 tubules from 5 random fields (100×) were evaluated for each animal. The positively and negatively stained proximal tubules were manually counted, and verified by an individual who was blinded to study design and animal identification numbers. The ratio of positively stained tubules to the total number of tubules was recorded.

**Enzyme-linked immunosorbent assay (ELISA) detection of KIM-1 protein.** Kidney levels of KIM-1 protein were determined by using a mouse TIM-1/KIM-1/HAVCR Quantikine ELISA Kit (R&D systems). Briefly, kidney tissue (10 mg) was homogenized in 1 ml of calibrator diluent RD5-26 buffer using Bead Ruptor 24 Elite (Omni International, Kennesaw, Georgia). The homogenate was centrifuged at 10 000 rpm for 5 min, and the supernatant was subject to ELISA detection of KIM-1 according to the manufacturer's instructions.

**Immunohistochemical detection of BrdU.** BrdU-positive cells were counted on paraffin-embedded sections using a commercially available kit (Invitrogen, Carlsbad, California). Each slide



contained a section of duodenum for positive control of BrdU incorporation. Five random fields (200 $\times$ ), or at least 500 tubular nuclei, were counted for each animal. The ratio of positively stained nuclei to total nuclei was determined for each animal. Results were verified by an individual who was blinded to study design and animal identification numbers.

**Quantitative reverse transcription real-time polymerase chain reaction (qRT-PCR).** qRT-PCR was carried out using 40 ng of kidney cDNA as previously described for liver tissue (Cichocki et al., 2017c). TaqMan probes (*Havcr1*: Mm00506686\_m1; *Fabp1*: Mm00444340\_m1; *Lcn2*: Mm01324470\_m1; *Tbp*: Mm01277042\_m1; Thermo Fisher Scientific) were used as per the manufacturer's instructions. Expression of *Tbp* was used as a reference.

**mRNA sequencing.** The protocol for mRNA sequencing has been previously described in Cichocki et al. (2017a). Briefly, cDNA libraries were generated from high-quality (RNA integrity number >8.0) RNA samples from RNA extracted from pulverized kidney tissue using an Illumina TruSeq mRNA stranded HT kit (Illumina, San Diego, California). An Illumina HT-2500 was used for sequencing; all samples were run on the same flow cell. After filtering and mapping to the GRcm38/mm10 assembly, a list of 20 032 genes was obtained. Differential gene expression was determined via the R (v 3.3.1) package DESeq2 (v 1.12.3) (Love et al., 2014). To be deemed differentially expressed,  $\log_2$  fold-changes and false discovery rate (FDR)-adjusted *p* values were cut off at .58 and .1, respectively. A cut-off for  $\log_2$  of 0.58 represents an approximate 1.5-fold change in expression level compared with the reference (LFD) group. Default settings in DESeq2 were used for FDR adjustment (Benjamini and Hochberg, 1995).

**Data analyses.** GraphPad Prism (v 5.0), was used for statistical analysis. One-way ANOVA followed by Newman-Keuls post hoc test was used for comparisons between dgroups, where a *p* value <.05 was deemed statistically significant. The area under the curve (AUC) of PERC metabolites was calculated by trapezoidal rule, where the observed period was 0–36 h for PERC and TCA, and 0–12 h for TCVG, TCVC, and NAcTCVC. The data points below detection limits were replaced by  $\frac{1}{2}$  LOD for the calculation of AUC, as recommended by US EPA (US EPA, 2000). For analysis of correlations between metabolizing enzyme transcript abundance and toxicokinetic phenotype, Pearson correlation coefficients were determined and associated *p* values were corrected for multiple comparisons (Benjamini and Hochberg, 1995).

**Data availability.** RNA sequencing data are publicly available through Gene Expression Omnibus (GEO: GSE115641). In addition to GEO, complete lists of differentially expressed genes and enriched pathways are provided as [Supplementary Files](#). Raw data for PERC and metabolite levels in kidney are available in [Supplementary Table 1](#).

## RESULTS

### NAFLD Affects the Toxicokinetics of PERC and Its Oxidative and Conjugative Metabolites

We first determined whether experimental NAFLD affects kidney toxicokinetics of parent compound (PERC), oxidative (TCA), and GSH conjugative (TCVG, TCVC, and NAcTCVC) metabolites up to 36 h after administration of a single oral dose of PERC

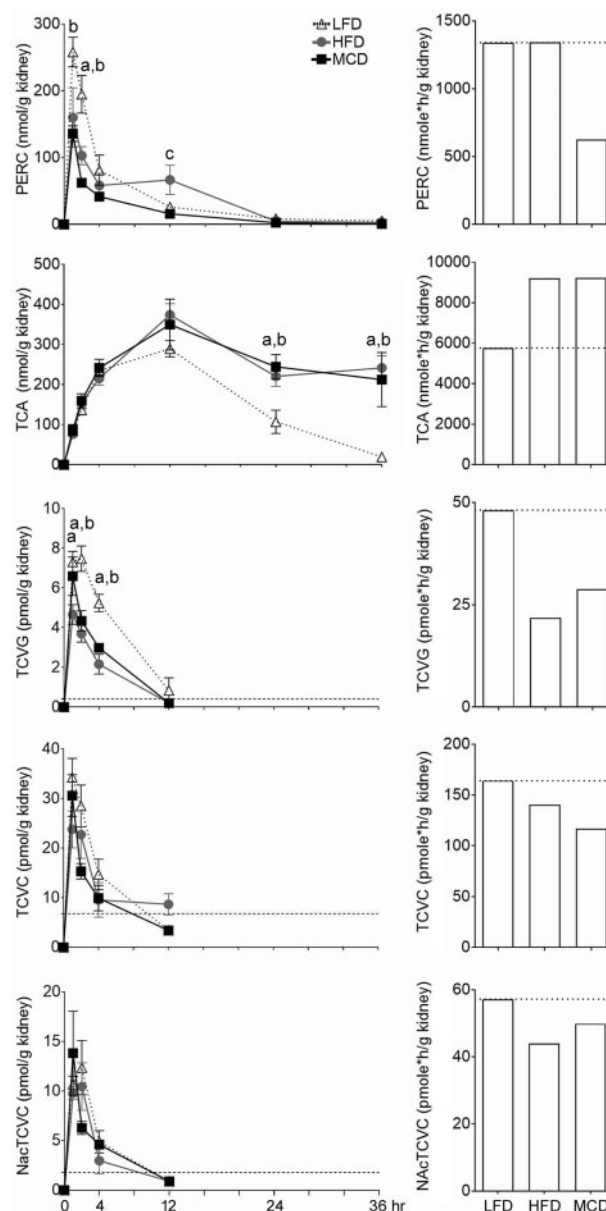


**Figure 2.** Kidney toxicokinetics of parent compound (PERC), oxidative metabolite (TCA), and glutathione conjugation metabolites of PERC (single dose, 300 mg/kg, i.g.) in male C57BL/6J mice fed with low-fat diet (LFD), high-fat diet (HFD), or methyl and choline deficient diet (MCD). Left panel shows the kinetic profiles, where the diet groups are identified by symbols (triangle, LFD; circle, HFD; square, MCD). Each dot is mean  $\pm$  SD (*n* = 4–5/time point/group). Individual animal data are available in [Supplementary Table 1](#). The dashed lines in line plots indicate the limit of detection (LOD) for each metabolite. Points below the limit of detection are plotted as  $\frac{1}{2}$  of the LOD as detailed in Materials and Methods section. Differences among groups at each time point were examined by one-way ANOVA with Newman-Keuls post hoc test, and are indicated by the letters to indicate significant differences (*p* < .05) as follows (a) LFD vs HFD, (b) LFD vs MCD, and (c) HFD vs MCD. Right panel indicates the area under the concentration-time curves (AUCs) that are derived from the group mean kinetic profiles of PERC metabolites up to 36 h after dosing. The dotted line indicates values for LFD-fed (control) group.

(300 mg/kg). The kidney kinetics of PERC was qualitatively similar among LFD-, HFD-, and MCD-fed mice (Figure 2, left panel). A comparison of differences among groups at each time point showed statistically significant effects for PERC, TCA, and TCVG, but not TCVC and NAcTCVC.

Table 1. Absolute Kidney Weight and Kidney to Bodyweight Ratios

	LFD		HFD		MCD	
	Vehicle	PERC	Vehicle	PERC	Vehicle	PERC
Absolute kidney weight	0.28 ± 0.03	0.30 ± 0.02	0.31 ± 0.02	0.31 ± 0.02	0.29 ± 0.01	0.30 ± 0.02
Kidney: BW ratio	1.07 ± 0.09 <sup>a</sup>	1.19 ± 0.08 <sup>b</sup>	0.90 ± 0.06 <sup>c</sup>	1.00 ± 0.03 <sup>a</sup>	1.01 ± 0.05 <sup>a</sup>	1.09 ± 0.07 <sup>a</sup>

Different superscripts indicate different statistical groups (ANOVA with Tukey's post hoc test;  $p < .05$ ).

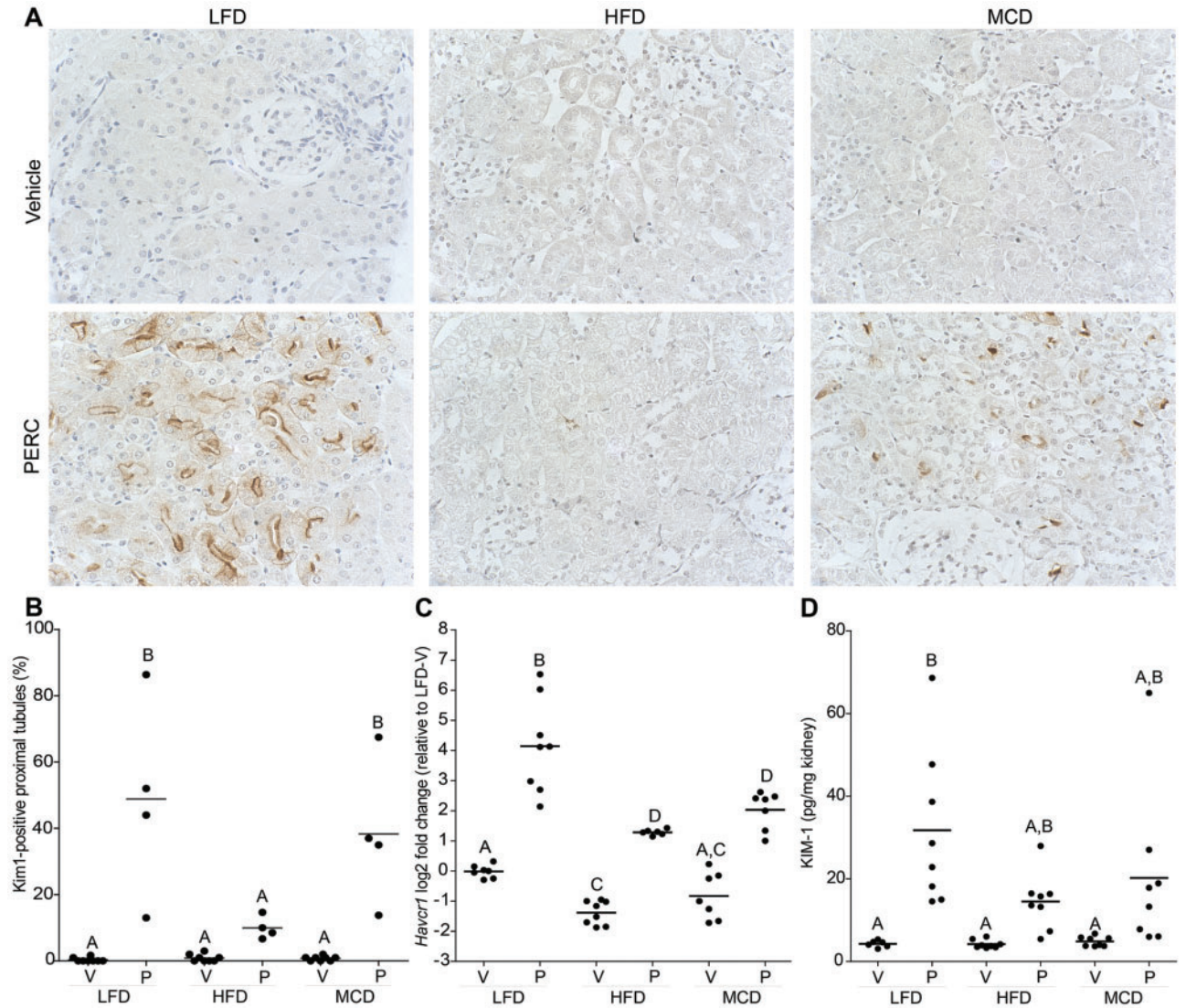


Figure 3. PERC-induced proximal tubular injury in mice after 8 weeks of low-fat diet (LFD), high-fat diet (HFD), or methyl and choline deficient diet (MCD). PERC-induced proximal tubular injury was visualized by staining for kidney injury molecule-1 (400 $\times$ ) (A). The percentage of positively stained proximal tubules (B), gene expression (C), and protein levels (D) of KIM-1 are shown in scatter plots (Abbreviations: V, Vehicle; P, PERC). Groups with different letters are significantly different (one-way ANOVA with Newman-Keuls post hoc test,  $p < .05$ ).

To evaluate the overall kinetics of each substance, area under the concentration-time curve (AUC) was plotted as bar graphs (Figure 2, right panel). MCD-fed mice had lower concentrations of PERC in the kidney, where AUC<sub>0-36h</sub> of PERC in MCD-fed mice was 47% of that in LFD-fed mice (Figure 2, top row). The AUC<sub>0-36h</sub> of TCA in the kidney was approximately 1.6-fold higher in HFD- and MCD-fed mice compared with LFD-fed mice, an apparent accumulation of TCA in the kidneys. Whereas the

results for PERC and TCA were interesting, perhaps the more toxicologically relevant finding was that mice with NAFLD had lower AUC<sub>0-12h</sub>s of TCVG, TCVG, and NAcTCVC in kidney tissue. Of particular note was the finding that the AUC<sub>0-12h</sub> of TCVG, which may be metabolically activated to electrophilic, cytotoxic, genotoxic, and/or mutagenic intermediates, was approximately 30%–40% lower in the kidneys of mice with NAFLD compared with LFD-fed mice.



### Biochemical and Histopathological Evaluation of Kidney Injury

Absolute kidney weight, but not kidney-to-bodyweight ratio, has been shown to correlate strongly with sub-chronic and chronic renal injury in rats (Craig et al., 2015). Absolute kidney weight was unaffected by diet or PERC exposure (Table 1); however, kidney-to-body weight ratio was decreased in HFD-fed mice compared with LFD-fed control, and was significantly increased by PERC exposure in all three diet groups. This effect was likely due to PERC causing about a 10% decrease in body weight (Cichocki et al., 2017b). There was no effect of diet or PERC exposure on BUN or serum creatinine levels. Histopathological assessment of PERC effects on the kidneys showed no pathological changes in either group (data not shown).

### HFD Manifests Protective Effects On Kidney Proximal Tubule Injury Caused by PERC

KIM-1 is a sensitive marker of acute renal injury and is especially useful for diagnosing xenobiotic-induced proximal tubular injury (Vaidya et al., 2008). We observed very few KIM-1-stained proximal tubules in vehicle-treated mice (Figure 3A). In PERC-exposed LFD- and MCD-fed mice, approximately 40%–50% of the proximal tubules were positively stained for KIM-1, indicating kidney injury, whereas only about 10% of the proximal tubules expressed detectable levels of KIM-1 in HFD-fed mice (Figure 3B). Data from immunohistochemical detection of KIM-1 were in concordance with gene expression of *Havcr1* (Figure 3C) and KIM-1 protein levels in kidney homogenates (Figure 3D).

### Effect of NAFLD On Mouse Kidney Transcriptome

To characterize the molecular effects of PERC exposure on the kidneys in mice with or without NAFLD we used RNA sequencing. First, we sought to understand the effect of HFD or MCD feeding on kidney gene expression in absence of PERC. Principal component analysis revealed that LFD-fed mice were completely separated from HFD- and MCD-fed mice, but the two NAFLD groups clustered together (Figure 4A). In HFD- or MCD-fed mice, a total of 223 and 165 genes, respectively, were differentially expressed compared with LFD-fed mice, with the majority of genes overlapping between these two groups (Figure 4B). There was a strong positive correlation between the gene expression data in HFD- and MCD-fed mice (Pearson's  $r = 0.80$ ), indicating that the directionality of change in expression (ie, up- or down-regulated) was similar between these two groups (Figure 4C). Molecular pathway analysis of the 125 genes that were differentially expressed in both HFD- and MCD-fed mice revealed altered retinol and drug metabolism and glycolysis/gluconeogenesis in the kidneys of mice with NAFLD (Table 2). With respect to genes involved in xenobiotic metabolism that were differentially expressed in HFD- of MCD-fed vehicle-treated mice (Figure 4D), we found that *Ces1g*, *Cyp2d12*, *Cyp2c68*, *Cyp2c69*, and *Slc22a29* were down-regulated in HFD- or MCD-fed mice. At the same time, *Slco1a1*, *Nat8f5*, *Ugt2b5*, and *Ugt2b37* were up-regulated compared with vehicle-treated LFD-fed mice. Generally, the effect of NAFLD on the expression of genes involved in xenobiotic metabolism was more pronounced in HFD- compared with MCD-fed mice.

### NAFLD-Dependent Perturbation of Kidney Lipid Metabolism in Mice Following PERC Exposure

PERC exposure was associated with differential expression of 378, 315, and 222 genes in kidneys of LFD-, HFD-, and MCD-fed mice, respectively. Of these genes, 109 overlapped among all three groups (Figure 5A). Gene set enrichment analysis revealed

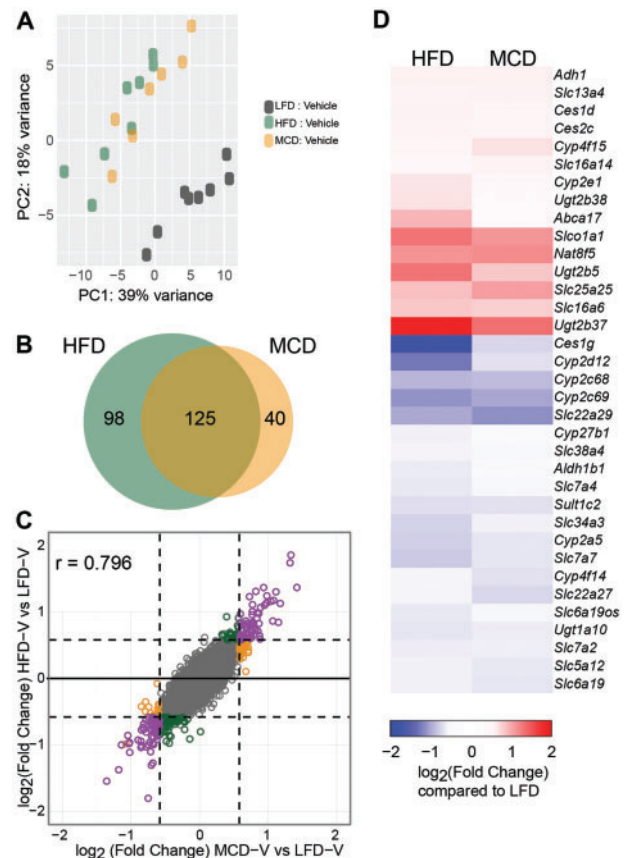


**Figure 4.** Effect of diets on kidney transcriptome. All analyses were conducted on vehicle-treated mice (24 h time point) after 8 weeks of low-fat diet (LFD), high-fat diet (HFD), or methyl and choline deficient diet (MCD). A, Principle component analysis of diet-mediated effects on kidney transcriptome. B, Venn diagram showing the differentially expressed genes of HFD or MCD group as compared with LFD group. Transcript with an absolute value of  $\log_2$  fold change  $> .58$  and an adjusted  $q$  value  $< .1$  is deemed to be differentially expressed. C, Plot of fold changes ( $\log_2$ , compared with LFD) of individual transcripts in HFD- and MCD-fed mice. Transcripts changed by diets are colored in green (HFD), orange (MCD), or purple (both). D, Heatmap of diet-associated effects on xenobiotic metabolism genes. Transcripts changed by diet are colored by red (up-regulation) or blue (down-regulation). See color images in the online version of the manuscript.

a number of molecular pathways in the kidneys were perturbed by PERC exposure, including fatty acid synthesis and metabolism, PPAR $\alpha$  signaling, and xenobiotic metabolism (Figure 5B), among which biosynthesis of unsaturated fatty acids and fatty acid metabolism were the most enriched pathways in MCD-fed mice. Whereas many pathways were enriched in all diet groups, a few PERC-dependent pathways were modulated in a diet-specific fashion. Xenobiotic metabolism and transport were enriched only in PERC-exposed LFD-fed mice, whereas butanoate metabolism and amino acid degradation were enriched only in PERC-exposed MCD-fed mice (Table 3).

Next, we extracted unique genes from the top five enriched pathways ('biosynthesis of unsaturated fatty acids,' 'fatty acid metabolism,' 'PPAR signaling pathways,' 'drug metabolism,' and 'metabolism of xenobiotics by cytochrome P450') and performed unsupervised hierarchical clustering of the individual genes (Figure 5C). Two anion transporter genes (*Slc7a13* and *Slc22a7*) were down-regulated in all PERC-treated animals. Metabolism-associated genes (*Ugt1a10*, *Ugt1a2*, *Aldh1b1*, and *Pck2*), amino acid transporter gene (*Slc43a1*), and Kim-1 gene (*Havcr1*) were up-regulated in PERC-treated mice; the effects were more

**Table 2.** Molecular Pathways Perturbed by HFD or MCD in Male C57BL/6J Mouse Kidney

KEGG PATHWAY	No. of Genes	Fold Enrichment	Benjamini Corrected q Value
<b>HFD: 223 genes</b>			
mmu01100: Metabolic pathways	33	2.2	8.56E-04
mmu00140: Steroid hormone biosynthesis	9	8.7	1.10E-03
mmu00830: Retinol metabolism	8	7.5	3.88E-03
mmu00983: Drug metabolism—other enzymes	6	9.9	9.20E-03
mmu00053: Ascorbate and aldarate metabolism	5	15.5	9.49E-03
mmu00980: Metabolism of xenobiotics by cytochrome P450	6	7.9	1.47E-02
mmu00982: Drug metabolism—cytochrome P450	6	7.6	1.52E-02
mmu00010: Glycolysis/gluconeogenesis	6	7.6	1.52E-02
mmu01130: Biosynthesis of antibiotics	10	3.9	1.64E-02
mmu00040: Pentose and glucuronate interconversions	5	11.7	1.67E-02
mmu05204: Chemical carcinogenesis	7	6.4	1.76E-02
mmu04610: Complement and coagulation cascades	6	6.6	2.59E-02
mmu00340: Histidine metabolism	4	14.0	3.26E-02
mmu04512: ECM-receptor interaction	6	5.7	4.13E-02
<b>MCD: 165 genes</b>			
mmu04610: Complement and coagulation cascades	9	12.9	4.63E-05
mmu00830: Retinol metabolism	7	8.6	9.44E-03
mmu00140: Steroid hormone biosynthesis	6	7.5	4.74E-02
mmu01100: Metabolic pathways	23	2.0	4.84E-02
<b>Common genes 125</b>			
mmu00830: Retinol metabolism	7	10.5	5.46E-03
mmu00140: Steroid hormone biosynthesis	6	9.2	2.58E-02
mmu01100: Metabolic pathways	21	2.2	2.06E-02
mmu00010: Glycolysis/gluconeogenesis	5	10.1	4.09E-02

pronounced in LFD-fed mice. The rest of xenobiotic metabolism-associated genes were also induced by PERC, but were more pronounced in HFD-fed mice. As a PPAR $\alpha$  responsive gene, *Cyp4a10* expression was induced by PERC in all three groups, with the greatest induction being observed in MCD- and HFD-fed mice compared with LFD-fed mice. The extent of *Cyp4a10* induction is concordant with the kidney levels of TCA, which is a known PPAR $\alpha$  activator. To confirm these diet-dependent effects of PERC on kidney gene expression that were discovered by RNA-sequencing, we measured the expression of *Lcn2*, *Havcr1*, and *Fabp1* via qRT-PCR. The results were largely similar between qRT-PCR (Supplementary Figs. 1A–C) and RNA-sequencing (Supplementary Figs. 1D–F).

## DISCUSSION

NAFLD is known to alter the expression of transporter and metabolism genes in the liver (Cichocki et al., 2017b; Clarke et al., 2014; Hardwick et al., 2014; Uno et al., 2018), which in turn can affect the delivered dose of xenobiotics to this organ (Cichocki et al., 2017a). Indeed, the differences in delivered dose depending on the liver disease state contributes to altered chemical-induced effects in the liver, as shown for benzo[a]pyrene (Uno et al., 2018), vinyl chloride (Lang et al., 2018), carbon tetrachloride (Donthamsetty et al., 2007), and PERC (Cichocki et al., 2017b). However, even though NAFLD has also been shown to affect the expression of renal xenobiotic transporters (Canet et al., 2015), few studies examined the effects of NAFLD on xenobiotic-induced renal injury (Hardwick et al., 2014). In this study, by using PERC as a model toxicant, we present several important findings on the effects of NAFLD on kidney metabolism and toxicity.

First, we show that NAFLD can modulate the metabolism and disposition of xenobiotics in the kidney. For example, HFD- or MCD-fed mice had greater TCA levels in kidney tissue compared with those in liver tissue (Cichocki et al., 2017a). Even though expression of hepatic genes associated with PERC oxidation (*Cyp2c29*, *Cyp3a11*, and *Cyp2b10*) was down-regulated in HFD- or MCD-fed mice (Cichocki et al., 2017b), we observed higher levels of TCA in liver and kidney tissue from HFD- or MCD-fed mice compared with LFD-fed mice. This effect is concordant with the observed transcriptional responses to PERC in HFD- or MCD-fed mice whereby transporters were up-regulated and increased reabsorption of TCA in kidney may contribute to the increased retention of TCA in liver and the decreased urinary elimination of TCA (Cichocki et al., 2017b). However, additional studies are needed to elucidate which transporters or physiochemical properties may explain the differences in TCA kinetics in the kidney.

We also found that levels of the PERC glutathione conjugation metabolites TCVG, TCVC, and NAcTCVC were lower in the kidney of HFD- or MCD-fed mice compared with LFD-fed mice, which is concordant with the levels of these metabolites previously measured in liver and urine (Cichocki et al., 2017a). The lower levels of glutathione conjugation metabolites are consistent with the repressed expression of GSTs in the liver of HFD- or MCD-fed mice compared with LFD-fed mice (Cichocki et al., 2017a). Notably, the tissue disposition of glutathione conjugation metabolites is qualitatively similar among LFD-, HFD-, and MCD-fed mice, where the most abundant metabolite is TCVG in liver and TCVC in kidney. The tissue-specific disposition of TCVG and TCVC is consistent with the results from previous studies (Luo et al., 2017). Collectively, these data suggest that the effect of liver disease state on the toxicokinetic properties of a xenobiotic is complex and involves hepatic and extrahepatic tissue (eg, kidney), chemical-physiological factors (eg, liver:





**Table 3.** Molecular Pathways Perturbed by PCE in Male C57BL/6J Mouse Kidney

KEGG PATHWAY LFD: 378 genes	No. of Genes	Enrichment	Benjamini q Value
mmu00980: Metabolism of xenobiotics by cytochrome P450	14	10.3	1.05E-07
mmu00982: Drug metabolism—cytochrome P450	14	10.0	7.88E-08
mmu01100: Metabolic pathways	58	2.1	4.04E-07
mmu03320: PPAR signaling pathway	14	8.2	4.70E-07
mmu00830: Retinol metabolism	14	7.4	1.42E-06
mmu00071: Fatty acid degradation	11	10.6	1.78E-06
mmu05204: Chemical carcinogenesis	14	7.2	1.53E-06
mmu01040: Biosynthesis of unsaturated fatty acids	6	10.5	5.40E-03
mmu00053: Ascorbate and aldarate metabolism	6	10.5	5.40E-03
mmu04146: Peroxisome	9	5.1	7.50E-03
mmu00140: Steroid hormone biosynthesis	9	4.9	9.30E-03
<b>HFD: 315 genes</b>			
mmu00071: Fatty acid degradation	15	14.2	1.85E-10
mmu00830: Retinol metabolism	14	7.3	4.52E-06
mmu00980: Metabolism of xenobiotics by cytochrome P450	12	8.7	6.10E-06
mmu03320: PPAR signaling pathway	13	7.5	5.63E-06
mmu01100: Metabolic pathways	54	2.0	2.48E-05
mmu00040: Pentose and glucuronate interconversions	9	11.6	2.36E-05
mmu01212: Fatty acid metabolism	10	9.1	3.20E-05
mmu00053: Ascorbate and aldarate metabolism	8	13.7	2.92E-05
mmu00982: Drug metabolism—cytochrome P450	10	7.0	2.30E-04
mmu00983: Drug metabolism—other enzymes	9	8.2	2.26E-04
mmu01040: Biosynthesis of unsaturated fatty acids	7	12.0	3.37E-04
mmu00860: Porphyrin and chlorophyll metabolism	8	9.0	3.83E-04
mmu05204: Chemical carcinogenesis	11	5.5	3.95E-04
mmu04610: Complement and coagulation cascades	10	6.1	4.73E-04
mmu00140: Steroid hormone biosynthesis	10	5.3	1.30E-03
mmu00062: Fatty acid elongation	6	10.7	2.49E-03
<b>MCD: 222 genes</b>			
mmu00071: Fatty acid degradation	14	20.2	1.10E-11
mmu01100: Metabolic pathways	43	2.4	1.63E-06
mmu03320: PPAR signaling pathway	11	9.7	7.77E-06
mmu00062: Fatty acid elongation	7	19.1	5.08E-05
mmu01040: Biosynthesis of unsaturated fatty acids	7	18.4	5.17E-05
mmu00830: Retinol metabolism	10	8.0	1.04E-04
mmu01212: Fatty acid metabolism	8	11.1	1.46E-04
mmu01130: Biosynthesis of antibiotics	13	4.3	8.60E-04
mmu04146: Peroxisome	8	6.8	2.82E-03

Third, the internal dosimetry of PERC and its metabolites agree with what is known and/or hypothesized about the target organ toxicity of PERC. For instance, the greater tissue levels of TCA in HFD- or MCD-fed mice concur with the more pronounced PPAR $\alpha$  activation in the liver and kidney of these mice compared with LFD-fed controls. Likewise, abrogation of proximal tubule injury from PERC in mice with NAFLD, particularly in HFD-fed mice, and a less pronounced effect of PERC on the kidney transcriptome in HFD and MCD mice, are also in line with reduced amounts of glutathione conjugates in these two groups as compared with LFD, particularly the significant effects on TCVC. These observations are in accord with the results from a study using cytochrome P450 2E1 (CYP2E1) knockout and humanized transgenic mice to investigate the metabolism and toxicity of PERC (Luo *et al.*, 2018a), in which CYP2E1 knockout mice exhibited lower TCVC, TCVC, and NaTCVC levels in kidney, which was associated with a milder PERC-induced proximal tubular injury as compared with wild-type mice. Even though glutathione conjugation metabolites of PERC represent a minor fraction of total metabolism, around 0.3% (Luo *et al.*,

2018b), their role in nephrotoxicity of PERC is well-established through formation of reactive sulfoxides (Cichocki *et al.*, 2016).

There are a number of limitations to this study. For example, animals were administered a relatively high dose of PERC (300 mg/kg, i.g.), which is unlikely to occur in humans. PERC oxidation is saturable at doses over 200 mg/kg (Buben and O'Flaherty, 1985), which may limit our interpretation for the kinetics observed in this study to those that occur at environmentally relevant exposures. However, the glutathione conjugation pathway is approximately 100-fold less efficient in mice compared with humans for the related compound trichloroethylene (Chiu *et al.*, 2009), therefore suggesting that the internal dose of glutathione metabolites in mouse kidney could still be relevant to PERC exposures to humans, albeit human data are not available and a PBPK model showed 1000-fold uncertainty in PERC glutathione conjugation (Chiu and Ginsberg, 2011). The other limitation of this study is the applicability of animal NAFLD/NASH models to human NAFLD, a contentious issue in the field (Maher, 2011; Teufel *et al.*, 2016). Even though HFD-fed animals can mimic the histopathological phenotype of human NAFLD, the degree of

injury depends on a number of factors including rodent strains (Lau et al., 2017). In addition, the metabolic profile of methionine/choline/folate-deficient (eg, MCD-fed) mice is different from human NASH (Rinella and Green, 2004) and is also dependent on rodent strain (Tryndyak et al., 2012). Despite these limitations, in this study we were able to characterize the effects of pre-existing liver disease on kidney metabolism and toxicity of PERC.

In summary, we confirmed that NAFLD can alter the internal dosimetry of PERC and its metabolites in kidney, which in turn affects PERC-induced nephrotoxicity in vivo. Whereas experimental NAFLD sensitized mice to PERC-induced liver toxicity (Cichocki et al., 2017b), we show here that NAFLD may be a protective factor for PERC-associated kidney effects due to reduced production and delivery of nephrotoxic glutathione conjugation-derived metabolites, as shown in male C57BL/6J fed HFD. However, this protective effect was abrogated in MCD-fed mice, which showed similarly decreased toxicokinetic sensitivity in the form of reduced nephrotoxic metabolite concentrations, but increased toxicodynamic sensitivity. These data, along with our previous study of how NAFLD affects liver toxicity (Cichocki et al., 2017b), demonstrate not only that underlying disease state could be an important factor to consider in future human health assessments of environmental toxicants, but also that the relationship between common diseases such as NAFLD and xenobiotic-induced toxicity may involve a complex, organ-specific interplay of toxicokinetic and toxicodynamic effects.

## SUPPLEMENTARY DATA

Supplementary data are available at Toxicological Sciences online.

## ACKNOWLEDGMENTS

The authors thank Dr Anthony H. Knap and Dr Terry Wade and Mr Stephen Sweet, Texas A&M University, for providing technical assistance on analytical chemistry analyses. The views expressed in this manuscript do not necessarily represent those of the U.S. Food and Drug Administration. The authors have nothing to disclose.

## FUNDING

J.A.C. was a recipient of a National Research Service Award through the National Institutes of Health (F32 ES026005). This work was supported, in part, by a cooperative agreement STAR RD83561202 from US Environmental Protection Agency (EPA) and by a grant from NIH (P42 ES005948) to Texas A&M University. The views expressed in this paper are those of the authors and do not necessarily reflect the views or policies of the NIH, EPA, or FDA.

## REFERENCES

- Benjamini, Y., and Hochberg, Y. (1995). Controlling the false discovery rate—A practical and powerful approach to multiple testing. *J. R. Stat. Soc. Ser. B: Methodol.* **57**, 289–300.
- Browning, J. D., Szczepaniak, L. S., Dobbins, R., Nuremberg, P., Horton, J. D., Cohen, J. C., Grundy, S. M., and Hobbs, H. H. (2004). Prevalence of hepatic steatosis in an urban population in the United States: Impact of ethnicity. *Hepatology* **40**, 1387–1395.
- Buben, J. A., and O'Flaherty, E. J. (1985). Delineation of the role of metabolism in the hepatotoxicity of trichloroethylene and perchloroethylene: A dose-effect study. *Toxicol. Appl. Pharmacol.* **78**, 105–122.
- Bull, R. J., Sanchez, I. M., Nelson, M. A., Larson, J. L., and Lansing, A. J. (1990). Liver tumor induction in B6C3F1 mice by dichloroacetate and trichloroacetate. *Toxicology* **63**, 341–359.
- Canet, M. J., Hardwick, R. N., Lake, A. D., Dzierlenga, A. L., Clarke, J. D., Goedken, M. J., and Cherrington, N. J. (2015). Renal xenobiotic transporter expression is altered in multiple experimental models of nonalcoholic steatohepatitis. *Drug Metab. Dispos.* **43**, 266–272.
- Chalasani, N., Younossi, Z., Lavine, J. E., Diehl, A. M., Brunt, E. M., Cusi, K., Charlton, M., and Sanyal, A. J. (2012). The diagnosis and management of non-alcoholic fatty liver disease: Practice Guideline by the American Association for the Study of Liver Diseases, American College of Gastroenterology, and the American Gastroenterological Association. *Hepatology* **55**, 2005–2023.
- Chiu, W. A., and Ginsberg, G. L. (2011). Development and evaluation of a harmonized physiologically based pharmacokinetic (PBPK) model for perchloroethylene toxicokinetics in mice, rats, and humans. *Toxicol. Appl. Pharmacol.* **253**, 203–234.
- Chiu, W. A., Okino, M. S., and Evans, M. V. (2009). Characterizing uncertainty and population variability in the toxicokinetics of trichloroethylene and metabolites in mice, rats, and humans using an updated database, physiologically based pharmacokinetic (PBPK) model, and Bayesian approach. *Toxicol. Appl. Pharmacol.* **241**, 36–60.
- Cichocki, J. A., Furuya, S., Konganti, K., Luo, Y. S., McDonald, T. J., Iwata, Y., Chiu, W. A., Threadgill, D. W., Pogribny, I. P., and Rusyn, I. (2017a). Impact of nonalcoholic fatty liver disease on toxicokinetics of tetrachloroethylene in mice. *J. Pharmacol. Exp. Ther.* **361**, 17–28.
- Cichocki, J. A., Furuya, S., Luo, Y. S., Iwata, Y., Konganti, K., Chiu, W. A., Threadgill, D. W., Pogribny, I. P., and Rusyn, I. (2017b). Nonalcoholic fatty liver disease is a susceptibility factor for perchloroethylene-induced liver effects in mice. *Toxicol. Sci.* **159**, 102–113.
- Cichocki, J. A., Furuya, S., Venkatratnam, A., McDonald, T. J., Knap, A. H., Wade, T., Sweet, S., Chiu, W. A., Threadgill, D. W., and Rusyn, I. (2017). Characterization of variability in toxicokinetics and toxicodynamics of tetrachloroethylene using the collaborative cross mouse population. *Environ. Health Perspect.* **125**, 057006.
- Cichocki, J. A., Guyton, K. Z., Guha, N., Chiu, W. A., Rusyn, I., and Lash, L. H. (2016). Target organ metabolism, toxicity, and mechanisms of trichloroethylene and perchloroethylene: Key similarities, differences, and data gaps. *J. Pharmacol. Exp. Ther.* **359**, 110–123.
- Clarke, J. D., Hardwick, R. N., Lake, A. D., Lickteig, A. J., Goedken, M. J., Klaassen, C. D., and Cherrington, N. J. (2014). Synergistic interaction between genetics and disease on pravastatin disposition. *J. Hepatol.* **61**, 139–147.
- Craig, E. A., Yan, Z., and Zhao, Q. J. (2015). The relationship between chemical-induced kidney weight increases and kidney histopathology in rats. *J. Appl. Toxicol.* **35**, 729–736.
- Cristofori, P., Sauer, A. V., and Trevisan, A. (2015). Three common pathways of nephrotoxicity induced by halogenated alkenes. *Cell Biol. Toxicol.* **31**, 1–13.
- Donthamsetty, S., Bhawe, V. S., Mitra, M. S., Latendresse, J. R., and Mehendale, H. M. (2007). Nonalcoholic fatty liver

- sensitizes rats to carbon tetrachloride hepatotoxicity. *Hepatology* **45**, 391–403.
- Elfarra, A. A., and Krause, R. J. (2007). S-(1, 2, 2-trichlorovinyl)-L-cysteine sulfoxide, a reactive metabolite of S-(1, 2, 2-trichlorovinyl)-L-cysteine formed in rat liver and kidney microsomes, is a potent nephrotoxicant. *J. Pharmacol. Exp. Ther.* **321**, 1095–1101.
- Hardwick, R. N., Clarke, J. D., Lake, A. D., Canet, M. J., Anumol, T., Street, S. M., Merrell, M. D., Goedken, M. J., Snyder, S. A., and Cherrington, N. J. (2014). Increased susceptibility to methotrexate-induced toxicity in nonalcoholic steatohepatitis. *Toxicol. Sci.* **142**, 45–55.
- Herren-Freund, S. L., Pereira, M. A., Khoury, M. D., and Olson, G. (1987). The carcinogenicity of trichloroethylene and its metabolites, trichloroacetic acid and dichloroacetic acid, in mouse liver. *Toxicol. Appl. Pharmacol.* **90**, 183–189.
- International Agency for Research on Cancer. (2014). *Trichloroethylene, Tetrachloroethylene and Some Other Chlorinated Agents*. WHO International Agency for Research on Cancer, Lyon, France.
- Japanese Industrial Safety Association. (1993). Carcinogenicity study of tetrachloroethylene by inhalation in rats and mice. Hadano, Japan.
- Jia, C., Yu, X., and Masiak, W. (2012). Blood/air distribution of volatile organic compounds (VOCs) in a nationally representative sample. *Sci. Total Environ.* **419**, 225–232.
- Kuhn, J. P., Meffert, P., Heske, C., Kromrey, M. L., Schmidt, C. O., Mensel, B., Volzke, H., Lerch, M. M., Hernando, D., Mayerle, J., et al. (2017). Prevalence of fatty liver disease and hepatic iron overload in a northeastern German population by using quantitative MR imaging. *Radiology* **284**, 706–716.
- Lang, A. L., Chen, L., Poff, G. D., Ding, W. X., Barnett, R. A., Arteel, G. E., and Beier, J. I. (2018). Vinyl chloride dysregulates metabolic homeostasis and enhances diet-induced liver injury in mice. *Hepatology* **67**, 270–284.
- Lash, L. H., and Parker, J. C. (2001). Hepatic and renal toxicities associated with perchloroethylene. *Pharmacol. Rev.* **53**, 177–208.
- Lau, J. K., Zhang, X., and Yu, J. (2017). Animal models of non-alcoholic fatty liver disease: Current perspectives and recent advances. *J. Pathol.* **241**, 36–44.
- Love, M. I., Huber, W., and Anders, S. (2014). Moderated estimation of fold change and dispersion for RNA-seq data with DESeq2. *Genome Biol.* **15**, 550.
- Luo, Y. S., Cichocki, J. A., McDonald, T. J., and Rusyn, I. (2017). Simultaneous detection of the tetrachloroethylene metabolites S-(1, 2, 2-trichlorovinyl) glutathione, S-(1, 2, 2-trichlorovinyl)-L-cysteine, and N-acetyl-S-(1, 2, 2-trichlorovinyl)-L-cysteine in multiple mouse tissues via ultra-high performance liquid chromatography electrospray ionization tandem mass spectrometry. *J. Toxicol. Environ. Health A* **80**, 513–524.
- Luo, Y. S., Furuya, S., Soldatov, V. Y., Kosyk, O., Yoo, H. S., Fukushima, H., Lewis, L., Iwata, Y., and Rusyn, I. (2018a). Metabolism and toxicity of trichloroethylene and tetrachloroethylene in cytochrome P450 2E1 knockout and humanized transgenic mice. *Toxicol. Sci.* **164**, 489–500.
- Luo, Y. S., Hsieh, N. H., Soldatov, V. Y., Chiu, W. A., and Rusyn, I. (2018b). Comparative analysis of metabolism of trichloroethylene and tetrachloroethylene among mouse tissues and strains. *Toxicology* **409**, 33–43.
- Machado, M. V., Michelotti, G. A., Xie, G., Almeida Pereira, T., Boursier, J., Bohnic, B., Guy, C. D., and Diehl, A. M. (2015). Mouse models of diet-induced nonalcoholic steatohepatitis reproduce the heterogeneity of the human disease. *PLoS One* **10**, e0127991.
- Maher, J. J. (2011). New insights from rodent models of fatty liver disease. *Antioxid. Redox Signal.* **15**, 535–550.
- Musso, G., Cassader, M., Cohney, S., Pinach, S., Saba, F., and Gambino, R. (2015). Emerging liver-kidney interactions in nonalcoholic fatty liver disease. *Trends Mol. Med.* **21**, 645–662.
- Musso, G., Gambino, R., Tabibian, J. H., Ekstedt, M., Kechagias, S., Hamaguchi, M., Hultcrantz, R., Hagstrom, H., Yoon, S. K., Charatcharoenwitthaya, P., et al. (2014). Association of non-alcoholic fatty liver disease with chronic kidney disease: A systematic review and meta-analysis. *PLoS Med.* **11**, e1001680.
- National Research Council. (2010). *Review of the Environmental Protection Agency's Draft IRIS Assessment of Tetrachloroethylene*. The National Academies Press, Washington, DC.
- National Toxicology Program. (1977). Bioassay of tetrachloroethylene for possible carcinogenicity. *Natl. Cancer Inst. Carcinog. Tech. Rep. Ser.* **13**, 1–83.
- National Toxicology Program. (1986). NTP toxicology and carcinogenesis studies of tetrachloroethylene (perchloroethylene) (CAS no. 127-18-4) in F344/N rats and B6C3F1 mice (inhalation studies). *Natl. Toxicol. Program Tech. Rep. Ser.* **311**, 1–197.
- Philip, B. K., Mumtaz, M. M., Latendresse, J. R., and Mehendale, H. M. (2007). Impact of repeated exposure on toxicity of perchloroethylene in Swiss Webster mice. *Toxicology* **232**, 1–14.
- Porta, E. A., Markell, N., and Dorado, R. D. (1985). Chronic alcoholism enhances hepatocarcinogenicity of diethylnitrosamine in rats fed a marginally methyl-deficient diet. *Hepatology* **5**, 1120–1125.
- Rinella, M. E., and Green, R. M. (2004). The methionine-choline deficient dietary model of steatohepatitis does not exhibit insulin resistance. *J. Hepatol.* **40**, 47–51.
- Rivkin, M., Simerzin, A., Zorde-Khvaleyevsky, E., Chai, C., Yuval, J. B., Rosenberg, N., Harari-Steinfeld, R., Schneider, R., Amir, G., Condiotti, R., et al. (2016). Inflammation-induced expression and secretion of microRNA 122 leads to reduced blood levels of kidney-derived erythropoietin and anemia. *Gastroenterology* **151**, 999–1010 e3.
- Roberti, M. F., Perazzo, J. C., and Monserrat, A. J. (1988). Effects of unilateral ureteric occlusion on renal necrosis occurring in rats fed a methyl-deficient diet. *Br. J. Exp. Pathol.* **69**, 449–456.
- Teufel, A., Itzel, T., Erhart, W., Brosch, M., Wang, X. Y., Kim, Y. O., von Schonfels, W., Herrmann, A., Bruckner, S., Stickel, F., et al. (2016). Comparison of gene expression patterns between mouse models of nonalcoholic fatty liver disease and liver tissues from patients. *Gastroenterology* **151**, 513–525 e0.
- Tryndyak, V. P., Latendresse, J. R., Montgomery, B., Ross, S. A., Beland, F. A., Rusyn, I., and Pogribny, I. P. (2012). Plasma microRNAs are sensitive indicators of inter-strain differences in the severity of liver injury induced in mice by a choline- and folate-deficient diet. *Toxicol. Appl. Pharmacol.* **262**, 52–59.
- Uno, S., Nebert, D. W., and Makishima, M. (2018). Cytochrome P450 1A1 (CYP1A1) protects against nonalcoholic fatty liver disease caused by Western diet containing benzo[a]pyrene in mice. *Food Chem. Toxicol.* **113**, 73–82.
- US EPA. (2000). *Guidance for Data Quality Assessment: Practical Methods for Data Analysis*. Washington, DC.
- U.S. EPA. (2011). Toxicological review of tetrachloroethylene (CAS no. 127-18-4). In *Support of Summary Information on the Integrated Risk Information System (IRIS)*. U.S. Environmental Protection Agency, Washington, DC.



- Vaidya, V. S., Ferguson, M. A., and Bonventre, J. V. (2008). Biomarkers of acute kidney injury. *Annu. Rev. Pharmacol. Toxicol.* **48**, 463–493.
- Younossi, Z. M., Blissett, D., Blissett, R., Henry, L., Stepanova, M., Younossi, Y., Racila, A., Hunt, S., and Beckerman, R. (2016a). The economic and clinical burden of nonalcoholic fatty liver disease in the United States and Europe. *Hepatology* **64**, 1577–1586.
- Younossi, Z. M., Koenig, A. B., Abdelatif, D., Fazel, Y., Henry, L., and Wymer, M. (2016b). Global epidemiology of nonalcoholic fatty liver disease—Meta-analytic assessment of prevalence, incidence, and outcomes. *Hepatology* **64**, 73–84.
- Zeise, L., Bois, F. Y., Chiu, W. A., Hattis, D., Rusyn, I., and Guyton, K. Z. (2013). Addressing human variability in next-generation human health risk assessments of environmental chemicals. *Environ. Health Perspect.* **121**, 23–31.
- Zelber-Sagi, S., Nitzan-Kaluski, D., Halpern, Z., and Oren, R. (2006). Prevalence of primary non-alcoholic fatty liver disease in a population-based study and its association with biochemical and anthropometric measures. *Liver Int.* **26**, 856–863.